Eur. J. Math. Appl. (2025)5:17 URL: http://ejma.euap.org

© 2025 European Journal of Mathematics and Applications

BIFURCATION, OPTICAL SOLUTIONS, AND MODULATION INSTABILITY ANALYSIS OF THE COMPLEX NONLINEAR (2+1)-DIMENSIONAL δ -POTENTIAL SCHRÖDINGER EQUATION

LAMA ABDULAZIZ ALHAKIM 1 , ADNAN AHMAD MAHMUD 2,* , ALAAEDDIN MOUSSA 1 , YAZID MATI 1 , BOUBEKEUR GASMI 3 , AND HACI MEHMET BASKONUS 4

ABSTRACT. This study conducts a thorough examination of the nonlinear (2+1)-dimensional time-space fractional Schrödinger equation associated with a δ -potential. Initially, bifurcation theory is employed to analyze the bifurcation, and the phase portrait of the solutions is subsequently investigated. Thereafter, the enhanced Cham technique is utilized to derive various types of traveling wave solutions, including periodic multi-wave solitons, condal waves, and kinks. Additionally, graphical representations of several obtained solutions are provided to facilitate a clearer understanding of the dynamic behaviors of the results. Furthermore, a linear stability analysis approach is introduced to perform an instability-modulated estimation for the model under scrutiny. The findings illustrate the effectiveness and versatility of our methodology in relation to other mathematical and physical models.

1. Introduction

In recent decades, mathematicians have focused on exploring complex phenomena in various fields of nonlinear sciences, including fluid dynamics, plasma physics, condensed matter physics, and others. As a result, many research studies have been conducted to describe these phenomena, particularly by using nonlinear evolution equations (NLEEs). Different types of NLEEs vary in their structures, properties, complexity, and practical applications. Various methods have been used in the literature to investigate these equations to obtain exact analytical solutions with different types and structures. Some of the most recent methods include the dual auxiliary equation technique, with its generalization [1–3], the expansion form of the fractional $\exp(-\Phi(\eta))$ technique that uses the Katugampola's fractional derivative [4], the Cham method [5] that generalizes several methods, the $\tanh(\eta)$ expansion method [6], the expansion form of sine-Gordon method [7], the extended direct algebraic method [8]. These approaches

¹Department of Management Information Systems and Production Management, College of Business & Economics, Qassim University, Buraidah, 51452, Saudi Arabia

 $^{^2\}mathrm{Department}$ of Mathematics, Faculty of Arts and Sciences, Harran University, 63290, Şanlurfa Türkiye

³Higher School of Management and Digital Economy, Kolea, Tipaza, Algeria

⁴Department of Mathematics and Science Education, Faculty of Education, Harran University, 63190, Şanliurfa, Türkiye

^{*}Corresponding author

 $[\]textit{E-mail addresses}. \ \texttt{4151@qu.edu.sa, mathematic79@yahoo.com, a.moussa@qu.edu.sa,}$

matie@qu.edu.sa, gasmiboubeker@gmail.com, 4hmbaskonus@gmail.com.

Key words and phrases. Nonlinear Schrödinger equation; Improved Cham method; Conformable operator; Instability modulation analysis.

have led to diverse solutions, including polynomial, exponential, rational, trigonometric, elliptic, and hyperbolic functions.

This paper investigates an essential and complex NLEE, namely the complex nonlinear (2+1)-dimensional time-space fractional Schrödinger's equation with the potential δ [9] (hereinafter referred to as δ -Schrödinger's equation), given in the following form:

(1)
$$i\mathcal{D}_t^{\alpha}\Xi + \frac{1}{2}\mathcal{D}_{xx}^{2\alpha}\Xi - a\delta\Xi - b \mid \Xi \mid^2 \Xi = 0,$$

where δ denotes the Dirac measure at the origin, a, b are non-zero constants, and \mathcal{D}^{α} indicates the conformable operators of order $0 < \alpha \le 1$, as promoted in [10], defined by:

(2)
$$\mathcal{D}_t^{\alpha}(f(t)) = \lim_{\varpi \to 0} \frac{f(t + \varpi t^{1-\alpha}) - f(t)}{\varpi}, \quad \forall t > 0, \quad 0 < \alpha \le 1.$$

The chain rule, which is the most significant instruction of the conformable operators, is organized as follows:

$$\mathcal{D}_{t}^{\alpha} f\left(g\left(t\right)\right) = f_{q}'[g\left(t\right)] \mathcal{D}_{t}^{\alpha}(g\left(t\right)).$$

This section first presents the previous works dealing with the δ -NLSE, then summarizes studies addressing the bifurcation theory, and finally provides the most recent research that has examined the modulation instability analysis of solutions to nonlinear equations. In Baleanu et al. [11], the enveloped complex form of the Ansatz function approach was applied to obtain bright and dark optical solitons. The extended version of the expansion sinh-Gordon equation method has been utilized in [9], led to the construction of diverse soliton solutions, including bright, dark-soliton combined forms of dark-bright soliton, and singular periodic traveling waves. The above two works also present some necessary conditions to certify the existence of the solutions. In Cheng et al. [12], the authors converted the δ -NLSE into a drift-admitting jump technique and proposed a novel second-order finite difference scheme to find some solutions that were validated using numerical examples. Deift et al. [13] employed the transformations of Backlünd to expand solutions from the half to the whole lines, and the nonlinear steepestdescent approach for Riemann-Hilbert problems has been employed to examine the stability of the stationary one-soliton solution. Additionally, the study in Li et al. [14] applied the generalized rational version of the exponential function approach to obtain complex, trigonometric, and hyperbolic soliton solutions. The authors in [15] employed the multi-symplectic Runge-Kutta-Nyström methods for analyzing the δ -NLSE. Moreover, [16] demonstrated that modified scattering and global solutions with decay in L^{∞} were produced from minimal starting data in a balanced Sobolev space. The authors of [17] illustrated how two solitons may separate from a soliton that is distributed by an outside δ -potential. The authors in [18] demonstrated, using the distorted Fourier transform, according to a certain compact asymmetrical pattern, a solution exists that converges to this small asymptotic profile. Besides, there are extra resources that provide details about different generation methods, and models [19–23]. Several researchers examined the bifurcation of the outcomes to explore the alterations in the overall framework of systems with dynamics as characteristics are varied. This bifurcation was used in [24] to discuss the dynamical actions of the Kodomtsev-Petviashvili equation, in [3] for the

nonlinear Schrödinger's equation in the recognize of conformable operator, in [25] for the unpredictable fraction Hirota–Maccari system, in [2] for the time-fractional nonlinear maccari's system, and in [5] for the (2+1)-multidimensional Bogoyavlenskii's breaking soliton problems.

The modulation instability analysis of solutions was examined in [26] for the (3+1)-dimensional nonlinear Schrödinger's equation, in [27] for the modify unstable NSE, in [28] for Radhakrishnan-Kundu-Lakshmanan model that has a coupled vector form, in [29] for the Lakshmanan-Porsezian- Daniel system with the parabolic rule of non-linearity, in [30] for the nonlinear Manakov-system, in [31] for the quadratic-cubic nonlinear Schrödinger's equation, and in [14] for the cubic NSE with repelling δ -potential. Different physical, mathematical, and engineering models have been investigated using semi-analytic methods [32–36], finally, the unified approach [37].

To summarize, some previous studies have explored the δ -NLSE, but none utilized the conformable operator we used in our research. The bifurcation concept was the main strategy utilized to explore the bifurcation and phase portrait of the results. Finally, only a few studies have looked into modulation instability analysis.

The rest of the work is arranged in the following manner: In Section 1, we present previous works dealing with the Schrödinger's equation. Section 2 presents the bifurcation and phase portrait of the solutions. Section 3 explains the steps of the improved Cham method followed in Section 4 by its application to find exact solutions to δ -Schrödinger's equation as well as the graphical representation of some obtained solutions to help readers better understand their propagation and features. Section 5 gives a study of instability modulation analysis of stationary solutions. Section 6 concludes the paper.

2. Bifurcation and phase portraits to δ -Schrödinger's equation

The present section discusses the bifurcation and phase profile of traveling wave solutions to δ -Schrödinger's equation. For this aim, we consider the following form of alteration:

(3)
$$\Xi(x,t) = \Theta(\eta)e^{i\psi}; \quad \eta = \left(\frac{x^{\alpha}}{\alpha} - p\frac{t^{\alpha}}{\alpha}\right); \quad \psi = \left(p\frac{x^{\alpha}}{\alpha} + r\frac{t^{\alpha}}{\alpha}\right),$$

where p and r are non-zero constants. Putting Eq. (3) into Eq. (1), we obtain:

(4)
$$i\left(-p\Theta'+ir\Theta\right)e^{i\psi}+\frac{1}{2}\left(\Theta''-p^2\Theta+i2p\Theta'\right)e^{i\psi}-a\delta\Theta-b\Theta^3e^{i\psi}=0,$$

which leads, after simplification, to Eq. (5) where "'" stands for $\frac{d}{d\xi}$.

(5)
$$\Theta'' - 2b\Theta^3 - (p^2 + 2(r + a\delta))\Theta = 0.$$

By setting $\Theta' = \phi$, we have the following planar system:

(6)
$$\begin{cases} \frac{d\Theta}{d\eta} = \phi, \\ \frac{d\phi}{d\eta} = 2b\Theta^3 + (p^2 + 2(r + a\delta))\Theta. \end{cases}$$

The Jacobian matrix $J(\Theta, \phi)$ is given by Eq. (7).

(7)
$$J(\Theta, \phi) = \begin{pmatrix} 0 & 1 \\ 6b\Theta^2 + p^2 + 2(r + a\delta) & 0 \end{pmatrix},$$

The characteristic polynomial of $J(\Theta, \phi)$ is $P(\lambda) = \lambda^2 - (6b\Theta^2 + p^2 + 2(r + a\delta))$. To evaluate the fixed points of system (6), we set $\frac{d\Theta}{d\eta} = 0$ and $\frac{d\phi}{d\eta} = 0$ For getting the subsequent pair of instances:

Case 1: Where b > 0 and $(p^2 + 2(r + a\delta)) > 0$, we have a fixed point $E_0(0,0)$. Since $P(\lambda) = \lambda^2 - (p^2 + 2(r + a\delta))$, the eigenvalues are:

$$\lambda_{12} = \pm \sqrt{p^2 + 2(r + a\delta)},$$

which implies that E_0 is a saddle point. Initially one of the eigenvalues is positive, we can deduce that the fixed point E_0 is unstable. Furthermore, there are a pair of homoclinic cycles at E_0 and Eq. (5) has two solitary wave solutions. Figure (1), generated using Maple 2022, depicts this example.

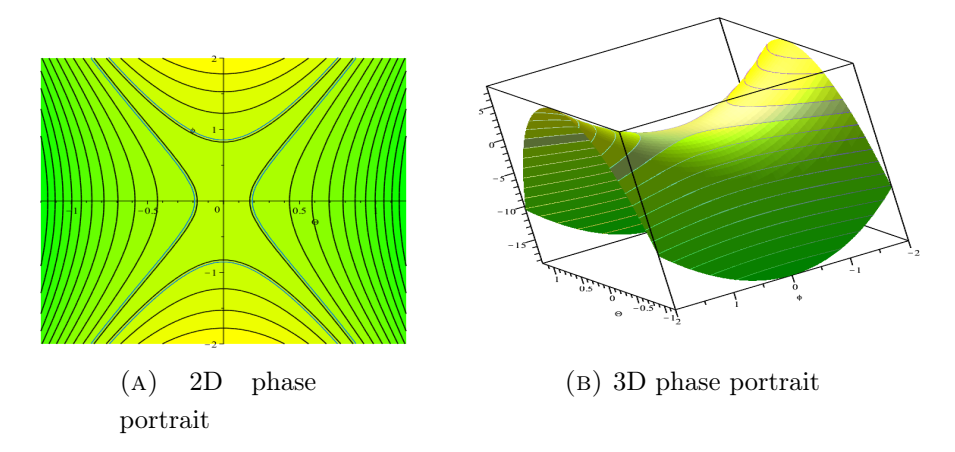


FIGURE 1. Phase portrait of system (6) when p = r = a = b = 1 and $\delta = 1$.

Case 2: Where b > 0 and $(p^2 + 2(r + a\delta)) < 0$, there are three fixed points $E_0(0,0)$, $E_1(\sqrt{-\frac{p^2 + 2(r + a\delta)}{2b}}, 0)$, and $E_2(-\sqrt{-\frac{p^2 + 2(r + a\delta)}{2b}}, 0)$. At $E_0(0,0)$, we have:

$$P(\lambda) = \lambda^2 - (p^2 + 2(r + a\delta)),$$

which in turn leads to:

$$\lambda_{1,2} = \pm i\sqrt{-(p^2 + 2(r + a\delta))}$$

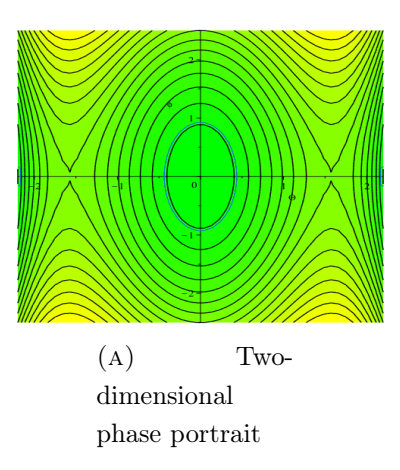
Therefore, E_0 is a center because λ_1 and λ_2 are two purely imaginary numbers and stable in the sense of Lyapunov.

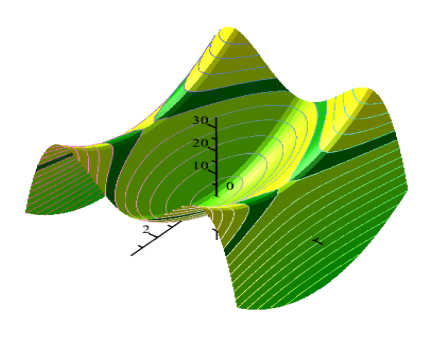
At the equilibrium points $(\Theta_e, \phi_e) = (\pm \sqrt{-\frac{p^2+2(r+a\delta)}{2b}}, 0)$, we have $P(\lambda) = \lambda^2 + 2(p^2 + 2(r+a\delta))$, leading to two eigenvalues:

$$\lambda_{1,2} = \pm \sqrt{-[p^2 + 2(r + a\delta)]},$$

which implies that we have two unstable saddle fixed points.

consequently, there is an assortment of periodic cycles at E_0 , two homoclinic cycles at $E_{1,2}$, and two series of bounded open orbits on the left (resp. right) sides at E_1 (resp. E_2). As a result, Eq. (5) has a collection of periodic wave solutions, two kink (anti-kink) wave solutions, and a series of breaking wave solutions. Figure (2), generated using Maple 2022, demonstrates this example.





(B) Three-dimensional phase portrait

FIGURE 2. Phases portrayal of system (6) when p = 1, r = -1, a = -2, b = 1, and $\delta = 1$.

3. The improved Cham method

In this section, we introduce the improved Cham method, an extension version of the Cham method recently proposed in [5], by describing its steps using the nonlinear partial differential equation given in Eq. (8):

(8)
$$F(\mathcal{J}, \mathcal{J}_t, \mathcal{J}_x, \mathcal{J}_{xt}, \mathcal{J}_{xx}, \mathcal{J}_{tt}, \cdots) = 0,$$

herein $\mathcal{J} = \mathcal{J}(x,t)$ is undetermined function.

Step 1. Use the transformation $\mathscr{J}(x,t) = G(\eta)$ with $\eta = x - vt$ to convert Eq. (8) to the following differential equation:

(9)
$$P\left(G, G_{\eta}, G_{\eta\eta}, G_{\eta\eta\eta}, \ldots\right) = 0.$$

Step 2. Express the solutions of Eq. (9) as a polynomial in $\left(\frac{\tanh(Z(\eta))}{\tanh(\eta)}\right)$ as follows:

(10)
$$G\left(\eta\right) = +\sum_{i=0}^{N} a_i \left(\frac{\tanh\left(Z(\eta)\right)}{\tanh\left(\eta\right)}\right)^i + \sum_{j=1}^{N} b_j \left(\frac{\tanh\left(Z(\eta)\right)}{\tanh\left(\eta\right)}\right)^{-j}; \quad a_N^2 + b_N^2 \neq 0,$$

where a_i , b_j (i, j = 0, 1, ..., N) are constant.

By applying the balancing declaration between the nonlinear terms, when the higher order has been equivalent to the greatest degree in Eq. (9), one directly fetches the value of the integer N. The term $\left(\frac{\tanh(Z(\eta))}{\tanh(\eta)}\right)$ satisfies the following differential equation :

(11)
$$\left(\frac{\tanh\left(Z(\eta)\right)}{\tanh\left(\eta\right)}\right)' = A\left(\frac{\tanh\left(Z(\eta)\right)}{\tanh\left(\eta\right)}\right)^2 + B\left(\frac{\tanh\left(Z(\eta)\right)}{\tanh\left(\eta\right)}\right) + C.$$

As a result, the following solutions can be obtained:

Family 1: When $4AC - B^2 > 0$ and $AC \neq 0$,

(12)

$$\left(\frac{\tanh\left(Z(\eta)\right)}{\tanh\left(\eta\right)}\right) = -\frac{B\tanh\left(\eta\right) + \tan\left(\frac{\sqrt{\tanh(\eta)^{2}(4AC - B^{2})}(\eta_{0} - \eta)}{2\tanh(\eta)}\right)\sqrt{\tanh\left(\eta\right)^{2}(4AC - B^{2})}}{2A\tanh\left(\eta\right)}, \quad \eta_{0} \in \mathbb{R}.$$

Family 2: When $4AC - B^2 < 0$ and $AC \neq 0$,

(13)

$$\left(\frac{\tanh\left(Z(\eta)\right)}{\tanh\left(\eta\right)}\right) = -\frac{B\tanh\left(\eta\right) - \tanh\left(\frac{\sqrt{\tanh(\eta)^{2}(B^{2} - 4AC)}(\eta_{0} - \eta)}{2\tanh(\eta)}\right)\sqrt{\tanh\left(\eta\right)^{2}(B^{2} - 4AC)}}{2A\tanh\left(\eta\right)}, \quad \eta_{0} \in \mathbb{R}$$

Family 3: When $4AC - B^2 = 0$ and AC > 0,

(14)
$$\left(\frac{\tanh\left(Z(\eta)\right)}{\tanh\left(\eta\right)}\right) = -\frac{2AC\xi^2 - 1 - \tanh\left(\frac{\ln(\eta) - \ln(AC\xi - \sqrt{AC}) + \eta_0}{2}\right)}{2A\xi\left(\sqrt{AC}\eta - 1\right)}, \quad \eta_0 \in \mathbb{R}.$$

Family 4: When A, B both are zero, and C be different from zero,

(15)
$$\left(\frac{\tanh(Z(\eta))}{\tanh(\eta)}\right) = \frac{C(\ln(\tanh(\eta) + 1) - \ln(\tanh(\eta) - 1))}{2} - \eta_0, \quad \eta_0 \in \mathbb{R}.$$

Family 5: When A, B both are non zero parameters, and C = 0,

(16)
$$\begin{cases} \left(\frac{\tanh(Z(\eta))}{\tanh(\eta)}\right) = -\frac{B(\exp(2\xi)-1)\exp(B\xi)}{\tanh(\eta)(A\exp(B\xi)-\eta_0)(\exp(2\xi)+1)}, & \eta_0 \in \mathbb{R}, \\ \eta \notin \left\{\frac{1}{B}\ln\left(\frac{\eta_0}{A}\right), 0\right\}, \left|\left(\frac{B(\exp(2\xi)-1)\exp(B\xi)}{(A\exp(B\xi)-\eta_0)(\exp(2\xi)+1)}\right| < 1. \end{cases}$$

Family 6: When A is different from zero, and B, C both are zero,

(17)
$$\left(\frac{\tanh(Z(\eta))}{\tanh(\eta)}\right) = \frac{1}{\eta_0 - A\xi}, \quad \eta_0 \in \mathbb{R}.$$

Family 7: When A is zero, and B, C are not zero,

(18)
$$\left(\frac{\tanh\left(Z(\eta)\right)}{\tanh\left(\eta\right)}\right) = -\frac{C + B\xi_0 \exp\left(B\xi\right)}{B}, \quad \eta_0 \in \mathbb{R}.$$

4. Exact solutions to δ -Schrödinger's equation

This section employs the improved Cham method to obtain semi-analytic solutions to Eq. (1). We start by utilizing the homogeneous balance between Θ^3 and Θ'' , from Eq. (5), to get the value N=1. This leads to solutions of Eq. (5) that take the following form:

(19)
$$\Theta(\eta) = b_1 \left(\frac{\tanh(Z(\eta))}{\tanh(\eta)} \right)^{-1} + a_0 + a_1 \left(\frac{\tanh(Z(\eta))}{\tanh(\eta)} \right),$$

where a_0 , a_1 and b_1 are constant, such that $a_1^2 + b_1^2 \neq 0$. By replacing Eq. (11), and Eq. (19) into Eq. (5), we can rehabilitate the left-hand side into some terms of $\left(\frac{\tanh(Z(\eta))}{\tanh(\eta)}\right)^j$, (j = 0, 1, 2, ...). Trying to organize separately the coefficient of the consequential polynomials and assign them to zero, to fetch an algebraic system of equations as follows:

$$\begin{cases}
(2A^{2}a_{1} - 2ba_{1}^{3}) = 0, \\
3ABa_{1} - 6ba_{0}a_{1}^{2} = 0, \\
2a_{1}\left(-3a_{1}b_{1}b + AC + \frac{B^{2}}{2} - 3a_{0}^{2}b - a\delta - \frac{p^{2}}{2} - r\right) = 0, \\
\left((BC - 12ba_{0}b_{1})a_{1} + Ab_{1}B - 2\left(a_{0}^{2}b + a\delta + \frac{p^{2}}{2} + r\right)a_{0}\right) = 0, \\
2b_{1}\left(-3a_{1}b_{1}b + AC + \frac{B^{2}}{2} - 3a_{0}^{2}b - a\delta - \frac{p^{2}}{2} - r\right) = 0, \\
(3BCb_{1} - 6ba_{0}b_{1}^{2}) = 0, \\
2C^{2}b_{1} - 2bb_{1}^{3} = 0.
\end{cases}$$

The algebraic system for b_1 , a_0 , a_1 , p, r, A, B and C, was solved using Maple 2022, to obtain the following solutions:

Family 1:

(21)
$$\left\{ r = AC - \frac{B^2}{4} - a\delta - \frac{p^2}{2}, \quad a_0 = \frac{B}{2\sqrt{b}}, \quad b_1 = \frac{C}{\sqrt{b}}, \quad a_1 = 0, \quad A = A, \quad B = B, \quad C = C \right\}$$

(22)
$$\Theta_1(\eta) = \frac{C}{\sqrt{b}} \left(\frac{\tanh(Z(\eta))}{\tanh(\eta)} \right)^{-1} + \frac{B}{2\sqrt{b}}.$$

Using Eq.(22) and solutions of Eq.(11), we obtain the following exact solutions of Eq.(1):

Case (1.1): When $4AC - B^2 > 0$ and $AC \neq 0$,

$$\begin{cases}
\Xi_{1.1}(\eta) = \left(\frac{C}{\sqrt{b}} \left(-\frac{B \tanh(\eta) + \tan\left(\frac{\sqrt{\tanh(\eta)^2(4AC - B^2)}(\eta_0 - \eta)}{2 \tanh(\eta)}\right) \sqrt{\tanh(\eta)^2(4AC - B^2)}}{2A \tanh(\eta)} \right)^{-1} + \frac{B}{2\sqrt{b}} \right) \times e^{i\psi} \\
\eta = \left(\frac{x^{\alpha}}{\alpha} - p\frac{t^{\alpha}}{\alpha}\right), \quad \psi = \left(p\frac{x^{\alpha}}{\alpha} + (AC - \frac{B^2}{4} - a\delta - \frac{p^2}{2})\frac{t^{\alpha}}{\alpha}\right), \quad \eta_0 \in \mathbb{R}.
\end{cases}$$
Case (1.2): When $4AC - B^2 < 0$ and $AC \neq 0$,
$$(24)$$

$$\begin{cases}
\Xi_{1.2}(\eta) = \left(\frac{C}{\sqrt{b}} \left(-\frac{B \tanh(\eta) - \tanh\left(\frac{\sqrt{\tanh(\eta)^2(B^2 - 4AC)}(\eta_0 - \eta)}{2 \tanh(\eta)}\right) \sqrt{\tanh(\eta)^2(B^2 - 4AC)}}{2A \tanh(\eta)}\right)^{-1} + \frac{B}{2\sqrt{b}}\right) \times e^{i\psi}, \\
\eta = \left(\frac{x^{\alpha}}{\alpha} - p\frac{t^{\alpha}}{\alpha}\right), \quad \psi = \left(p\frac{x^{\alpha}}{\alpha} + (AC - \frac{B^2}{4} - a\delta - \frac{p^2}{2})\frac{t^{\alpha}}{\alpha}\right), \quad \eta_0 \in \mathbb{R}.
\end{cases}$$

Case (1.3): When $4AC - B^2 = 0$ and AC > 0,

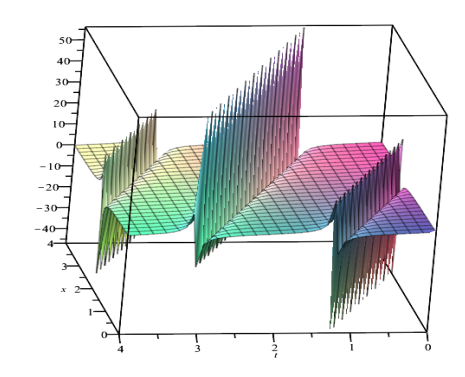
(25)
$$\begin{cases} \Xi_{1.3}(\eta) = \left(\frac{C}{\sqrt{b}} \left(-\frac{2AC\xi^2 - 1 - \tanh\left(\frac{\ln(\eta) - \ln(AC\xi - \sqrt{AC}) + \eta_0}{2}\right)}{2A\xi(\sqrt{AC}\eta - 1)}\right)^{-1} + \frac{B}{2\sqrt{b}}\right) \times e^{i\psi}, \\ \eta = \left(\frac{x^{\alpha}}{\alpha} - p\frac{t^{\alpha}}{\alpha}\right), \quad \psi = \left(p\frac{x^{\alpha}}{\alpha} + \left(-a\delta - \frac{p^2}{2}\right)\frac{t^{\alpha}}{\alpha}\right), \quad \eta_0 \in \mathbb{R}. \end{cases}$$

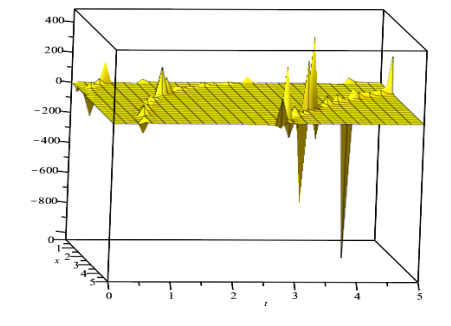
Case (1.4): When A = 0, B = 0 and $C \neq 0$,

(26)
$$\begin{cases} \Xi_{1.4}(\eta) = \left(\frac{C}{\sqrt{b}} \left(\frac{\tanh(Z(\eta))}{\tanh(\eta)}\right)^{-1}\right) \times e^{i\psi}, \\ \eta = \left(\frac{x^{\alpha}}{\alpha} - p\frac{t^{\alpha}}{\alpha}\right), \quad \psi = \left(p\frac{x^{\alpha}}{\alpha} + (-a\delta - \frac{p^{2}}{2})\frac{t^{\alpha}}{\alpha}\right), \quad \eta_{0} \in \mathbb{R}. \end{cases}$$

Case (1.5): When $A = 0, B \neq 0$ and $C \neq 0$,

(27)
$$\begin{cases} \Xi_{1.5}(\eta) = \left(\frac{C}{\sqrt{b}} \left(-\frac{C + B\xi_0 \exp(B\xi)}{B}\right)^{-1} + \frac{B}{2\sqrt{b}}\right) \times e^{i\psi}, \\ \eta = \left(\frac{x^{\alpha}}{\alpha} - p\frac{t^{\alpha}}{\alpha}\right), \quad \psi = \left(p\frac{x^{\alpha}}{\alpha} + \left(-\frac{B^2}{4} - a\delta - \frac{p^2}{2}\right)\frac{t^{\alpha}}{\alpha}\right), \quad \eta_0 \in \mathbb{R}. \end{cases}$$

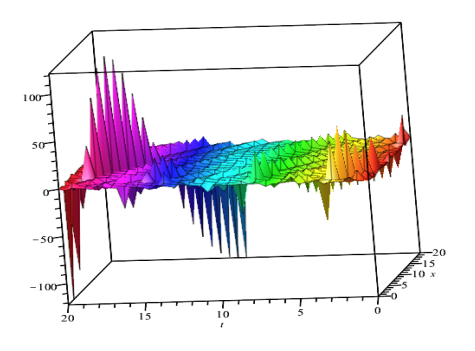


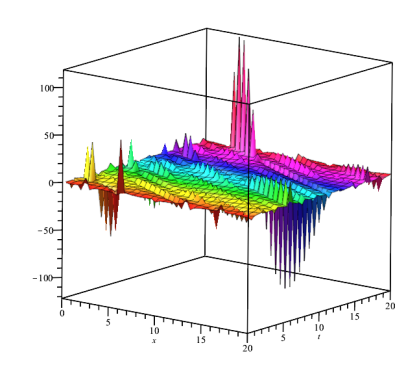


(A) Three-dimensional real-part

 $\hbox{$(B)$ Three-dimensional imaginary-part}$

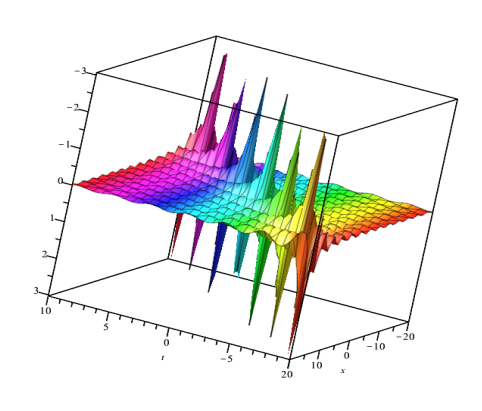
FIGURE 3. Absolute value of $\Xi_{1.1}(\eta)$ when $A=1, B=1, C=1, \eta_0=2, p=-2, b=1$, and $\alpha=\frac{1}{3}$ (kink wave solution).

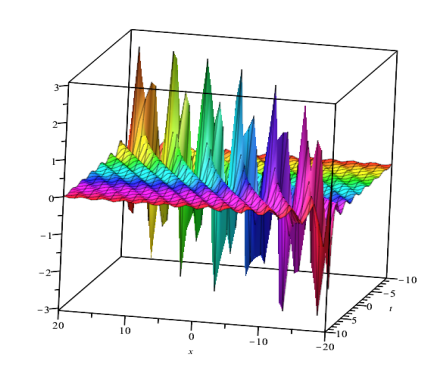




- (A) Three-dimensional real-part
- $\begin{array}{ll} {\rm (B)} & {\rm Three-dimensional} \\ {\rm imaginary-part} \end{array}$

FIGURE 4. Real and imaginary parts of $\Xi_{1.1}(\eta)$ when $A=1, B=1, C=1, \eta_0=2, p=-2, b=1$, and $\alpha=\frac{1}{3}$ (periodic multi-wave solitons).





- (A) Three-dimensional real-part
- $\begin{array}{ll} \text{(B)} & \text{Three-dimensional} \\ \text{imaginary-part} \end{array}$

FIGURE 5. Real and imaginary figures for $\Xi_{1.3}(\eta)$ when $A=2, C=2, \eta_0=2, p=-2, b=1, a=0.2, \delta=0.3$ and $\alpha=1$ (kinky-periodic lump wave).

Family 2:

(28)
$$\left\{ r = AC - \frac{B^2}{4} - a\delta - \frac{p^2}{2}, \quad b_1 = 0, \quad a_0 = \frac{B}{2\sqrt{b}}, \quad a_1 = \frac{A}{\sqrt{b}}, \quad A = A, \quad B = B, \quad C = C \right\}$$

(29)
$$\Theta_{2}(\eta) = \frac{B}{2\sqrt{b}} + \frac{A}{\sqrt{b}} \left(\frac{\tanh(Z(\eta))}{\tanh(\eta)} \right).$$

Using Eq.(28) and solutions of Eq.(11), the following exact solutions to Eq.(1) are achieved:

Case (2.1): When $4AC - B^2 > 0$ and $AC \neq 0$,

Case (2.1): When
$$4AC - B^2 > 0$$
 and $AC \neq 0$,
$$\begin{cases}
\Xi_{2.1}(\eta) = \left(\frac{B}{2\sqrt{b}} + \frac{A}{\sqrt{b}} \left(-\frac{B \tanh(\eta) + \tan\left(\frac{\sqrt{\tanh(\eta)^2(4AC - B^2)}(\eta_0 - \eta)}{2 \tanh(\eta)}\right) \sqrt{\tanh(\eta)^2(4AC - B^2)}}{2A \tanh(\eta)} \right) \right) \times e^{i\psi}, \\
\eta = \left(\frac{x^{\alpha}}{\alpha} - p\frac{t^{\alpha}}{\alpha}\right), \quad \psi = \left(p\frac{x^{\alpha}}{\alpha} + (AC - \frac{B^2}{4} - a\delta - \frac{p^2}{2})\frac{t^{\alpha}}{\alpha}\right), \quad \eta_0 \in \mathbb{R}.
\end{cases}$$
Case (2.2): When $4AC - B^2 < 0$ and $AC \neq 0$,
$$\begin{cases}
A \sqrt{\tanh(\eta)^2(B^2 - 4AC)}(\eta_0 - \eta)}, \quad \phi = \frac{1}{2} \left(\frac{A}{2} - \frac{A}{2} + \frac$$

Case (2.2): When $4AC - B^2 < 0$ and $AC \neq$

$$\begin{cases}
\Xi_{2.2}(\eta) = \left(\frac{B}{2\sqrt{b}} + \frac{A}{\sqrt{b}} \left(-\frac{B \tanh(\eta) - \tanh\left(\frac{\sqrt{\tanh(\eta)^2(B^2 - 4AC)}(\eta_0 - \eta)}{2\tanh(\eta)}\right) \sqrt{\tanh(\eta)^2(B^2 - 4AC)}}{2A \tanh(\eta)} \right) \right) \times e^{i\psi}, \\
\eta = \left(\frac{x^{\alpha}}{\alpha} - p\frac{t^{\alpha}}{\alpha}\right), \quad \psi = \left(p\frac{x^{\alpha}}{\alpha} + (AC - \frac{B^2}{4} - a\delta - \frac{p^2}{2})\frac{t^{\alpha}}{\alpha}\right), \quad \eta_0 \in \mathbb{R}.
\end{cases}$$

Case (2.3): When $4AC - B^2 = 0$ and AC > 0,

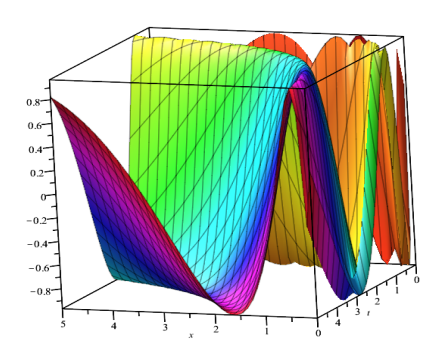
(32)
$$\begin{cases} \Xi_{2.3}\left(\eta\right) = \left(\frac{B}{2\sqrt{b}} + \frac{A}{\sqrt{b}}\left(-\frac{2AC\xi^2 - 1 - \tanh\left(\frac{\ln(\eta) - \ln(AC\xi - \sqrt{AC}) + \eta_0}{2}\right)}{2A\xi\left(\sqrt{AC}\eta - 1\right)}\right)\right) \times e^{i\psi}, \\ \eta = \left(\frac{x^{\alpha}}{\alpha} - p\frac{t^{\alpha}}{\alpha}\right), \quad \psi = \left(p\frac{x^{\alpha}}{\alpha} + \left(-a\delta - \frac{p^2}{2}\right)\frac{t^{\alpha}}{\alpha}\right), \quad \eta_0 \in \mathbb{R}. \end{cases}$$
Case (2.4): $A \neq 0$ $B = 0$ and $C = 0$

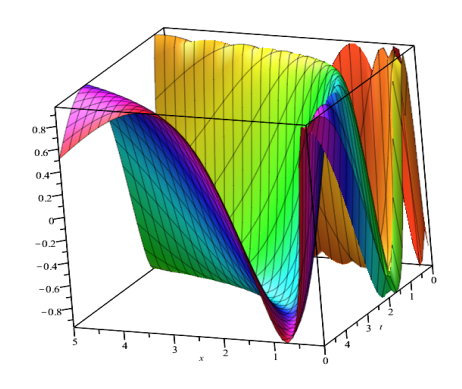
Case (2.4): $A \neq 0, B = 0$ and C = 0

Case (2.4):
$$A \neq 0, B = 0$$
 and $C = 0$,
$$\begin{cases}
\Xi_{2.4}(\eta) = \frac{A}{\sqrt{b}} \left(\frac{1}{\eta_0 - A\xi}\right) \times e^{i\psi}, \\
\eta = \left(\frac{x^{\alpha}}{\alpha} - p\frac{t^{\alpha}}{\alpha}\right), \quad \psi = \left(p\frac{x^{\alpha}}{\alpha} + (-a\delta - \frac{p^2}{2})\frac{t^{\alpha}}{\alpha}\right), \quad \eta_0 \in \mathbb{R}.
\end{cases}$$
Case (2.5): $A \neq 0, B \neq 0$ and $C = 0$,

Case (2.5): $A \neq 0, B \neq 0$ and C = 0.

(34)
$$\left\{ \begin{array}{l} \Xi_{2.5} \left(\eta \right) = \left(\frac{B}{2\sqrt{b}} + \frac{A}{\sqrt{b}} \left(-\frac{B(\exp(2\xi) - 1) \exp(B\xi)}{\tanh(\eta)(A \exp(B\xi) - \eta_0)(\exp(2\xi) + 1)} \right) \right) \times e^{i\psi}, \\ \eta \notin \left\{ \frac{1}{B} \ln \left(\frac{\eta_0}{A} \right), 0 \right\}, \left| \left(\frac{B(\exp(2\xi) - 1) \exp(B\xi)}{(A \exp(B\xi) - \eta_0)(\exp(2\xi) + 1)} \right| < 1, \quad \eta_0 \in \mathbb{R} \right. \end{array} \right.$$





- (A) Three-dimensional realpart
- (B) Three-dimensional imaginary-part

FIGURE 6. Real and imaginary profiles of $\Xi_{2.2}(\eta)$) when $A = \frac{1}{4}, B = 2, C = 1, \eta_0 = 2, p = -2, b = 0.8$, and $\alpha = \frac{1}{8}$ (coindal wave solutions).

Family 3:

(35)
$$\left\{ r = \frac{-(4AC + 2a\delta + p^2)}{2}, \quad a_0 = 0, \quad a_1 = \frac{A}{\sqrt{b}}, \quad b_1 = \frac{C}{\sqrt{b}}, \quad A = A, \quad B = 0, \quad C = C \right\}$$

(36)
$$\Theta_{3}(\eta) = \frac{C}{\sqrt{b}} \left(\frac{\tanh(Z(\eta))}{\tanh(\eta)} \right)^{-1} + \frac{A}{\sqrt{b}} \left(\frac{\tanh(Z(\eta))}{\tanh(\eta)} \right).$$

Using Eq.(36) and solutions of Eq.(11), we obtain the following exact solutions of Eq.(1):

Case (3.1): When $4AC - B^2 > 0$ and $AC \neq 0$,

$$\begin{cases}
\frac{C}{\sqrt{b}} \left(-\frac{\tan\left(\frac{\sqrt{\tanh(\eta)^{2}(4AC)}(\eta_{0} - \eta)}{2\tanh(\eta)}\right)\sqrt{\tanh(\eta)^{2}(4AC)}}{2A\tanh(\eta)} \right)^{-1} + \\
\frac{A}{\sqrt{b}} \left(-\frac{\tan\left(\frac{\sqrt{\tanh(\eta)^{2}(4AC)}(\eta_{0} - \eta)}{2\tanh(\eta)}\right)\sqrt{\tanh(\eta)^{2}(4AC)}}{2A\tanh(\eta)} \right) \\
\eta = \left(\frac{x^{\alpha}}{\alpha} - p\frac{t^{\alpha}}{\alpha}\right), \quad \psi = \left(p\frac{x^{\alpha}}{\alpha} - \left(\frac{4AC + 2a\delta + p^{2}}{2}\right)\frac{t^{\alpha}}{\alpha}\right), \quad \eta_{0} \in \mathbb{R}.
\end{cases}$$

Case (3.2): When $4AC - B^2 < 0$ and $AC \neq 0$

$$\begin{cases}
\frac{C}{\sqrt{b}} \left(-\frac{\tanh\left(\frac{\sqrt{\tanh(\eta)^{2}(-4AC)}(\eta_{0}-\eta)}{2\tanh(\eta)}\right)\sqrt{\tanh(\eta)^{2}(-4AC)}}{2A\tanh(\eta)} \right)^{-1} + \\
\frac{A}{\sqrt{b}} \left(-\frac{\tanh\left(\frac{\sqrt{\tanh(\eta)^{2}(-4AC)}(\eta_{0}-\eta)}{2\tanh(\eta)}\right)\sqrt{\tanh(\eta)^{2}(-4AC)}}{2A\tanh(\eta)} \right) \\
\eta = \left(\frac{x^{\alpha}}{\alpha} - p\frac{t^{\alpha}}{\alpha}\right), \quad \psi = \left(p\frac{x^{\alpha}}{\alpha} - \left(\frac{4AC + 2a\delta + p^{2}}{2}\right)\frac{t^{\alpha}}{\alpha}\right), \quad \eta_{0} \in \mathbb{R}.
\end{cases}$$

Case (3.3): When A = 0, B = 0 and $C \neq 0$,

(39)
$$\begin{cases} \Xi_{3.3}(\eta) = \frac{C}{\sqrt{b}} \left(\frac{C(\ln(\tanh(\eta)+1)-\ln(\tanh(\eta)-1))}{2} - \eta_0 \right)^{-1} \times e^{i\psi}, \\ \eta = \left(\frac{x^{\alpha}}{\alpha} - p \frac{t^{\alpha}}{\alpha} \right), \quad \psi = \left(p \frac{x^{\alpha}}{\alpha} - \left(\frac{2a\delta + p^2}{2} \right) \frac{t^{\alpha}}{\alpha} \right), \quad \eta_0 \in \mathbb{R}. \end{cases}$$

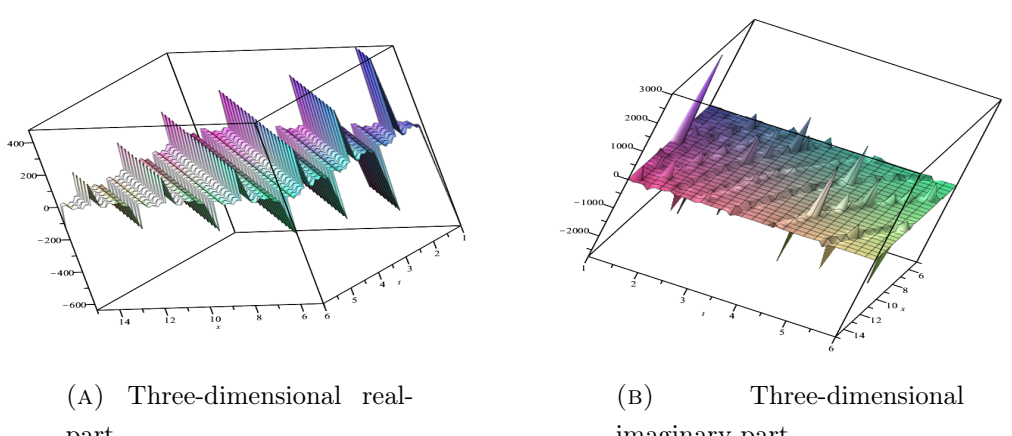
Case (3.4): $A \neq 0, B = 0$ and C = 0,

Case (3.4):
$$A \neq 0, B = 0$$
 and $C = 0$,
$$\begin{cases}
\exists 3.4 \ (\eta) = \frac{A}{\sqrt{b}} \left(\frac{1}{\eta_0 - A\xi}\right) \times e^{i\psi}, \\
\eta = \left(\frac{x^{\alpha}}{\alpha} - p\frac{t^{\alpha}}{\alpha}\right), \quad \psi = \left(p\frac{x^{\alpha}}{\alpha} - \left(\frac{2a\delta + p^2}{2}\right)\frac{t^{\alpha}}{\alpha}\right), \quad \eta_0 \in \mathbb{R}.
\end{cases}$$
Case (3.5): $A \neq 0, B \neq 0$ and $C = 0$,
$$\begin{cases}
(41) & \text{Case } \left(S.\left(\frac{x^{\alpha}}{\alpha} - p\frac{t^{\alpha}}{\alpha}\right), \quad \psi = \left(p\frac{x^{\alpha}}{\alpha} - \left(\frac{2a\delta + p^2}{2}\right)\frac{t^{\alpha}}{\alpha}\right), \quad \eta_0 \in \mathbb{R}.
\end{cases}$$

Case (3.5): $A \neq 0, B \neq 0$ and C = 0,

Ease (3.5):
$$A \neq 0, B \neq 0$$
 and $C = 0$,

41)
$$\begin{cases}
\Xi_{3.5}(\eta) = \left(\frac{C}{\sqrt{b}} \left(-\frac{B(\exp(2\xi) - 1) \exp(B\xi)}{\tanh(\eta)(A \exp(B\xi) - \eta_0)(\exp(2\xi) + 1)} \right)^{-1} + \frac{A}{\sqrt{b}} \left(-\frac{B(\exp(2\xi) - 1) \exp(B\xi)}{\tanh(\eta)(A \exp(B\xi) - \eta_0)(\exp(2\xi) + 1)} \right) \right) \times e^{i\psi}, \\
\eta \notin \left\{ \frac{1}{B} \ln \left(\frac{\eta_0}{A} \right), 0 \right\}, \left| \left(\frac{B(\exp(2\xi) - 1) \exp(B\xi)}{(A \exp(B\xi) - \eta_0)(\exp(2\xi) + 1)} \right| < 1, \quad \eta_0 \in \mathbb{R} \right\}
\end{cases}$$



part

imaginary-part

FIGURE 7. Absolute value of $\Xi_{3.1}(\eta)$) when $A=2, C=4, \eta_0=2, p=-2, b=0$ 0.8, and $\alpha = 1$ (resp. $\alpha = \frac{1}{9}$) (periodic singular solution).

Family 4:

$$\left\{ r = \frac{-(-8AC + 2a\delta + p^2)}{2}, \quad a_0 = 0, \quad a_1 = \frac{A}{\sqrt{b}}, \quad b_1 = -\frac{C}{\sqrt{b}}, \quad A = A, \quad B = 0, \quad C = C \right\}$$

(43)
$$\Theta_4(\eta) = -\frac{C}{\sqrt{b}} \left(\frac{\tanh(Z(\eta))}{\tanh(\eta)} \right)^{-1} + \frac{A}{\sqrt{b}} \left(\frac{\tanh(Z(\eta))}{\tanh(\eta)} \right).$$

Using Eq.(43) and solutions of Eq.(11), we obtain the following exact solutions of Eq.(1):

Case (4.1): When $4AC - B^2 > 0$ and $AC \neq 0$,

$$\begin{cases}
\frac{-C}{\sqrt{b}} \left(-\frac{\tan\left(\frac{\sqrt{\tanh(\eta)^{2}(4AC)}(\eta_{0}-\eta)}{2\tanh(\eta)}\right)\sqrt{\tanh(\eta)^{2}(4AC)}}{2A\tanh(\eta)} \right)^{-1} + \\
\Xi_{4.1}(\eta) = \begin{cases}
\frac{A}{\sqrt{b}} \left(-\frac{\tan\left(\frac{\sqrt{\tanh(\eta)^{2}(4AC)}(\eta_{0}-\eta)}{2\tanh(\eta)}\right)\sqrt{\tanh(\eta)^{2}(4AC)}}{2\tanh(\eta)} \right) \\
\eta = \left(\frac{x^{\alpha}}{\alpha} - p\frac{t^{\alpha}}{\alpha}\right), \quad \psi = \left(p\frac{x^{\alpha}}{\alpha} - \frac{(-8AC + 2a\delta + p^{2})}{2}\frac{t^{\alpha}}{\alpha}\right), \quad \eta_{0} \in \mathbb{R}.
\end{cases}$$
Case (4.2): When $AAC = P^{2} < 0$ and $AC \neq 0$.

Case (4.2): When $4AC - B^2 < 0$ and $AC \neq 0$,

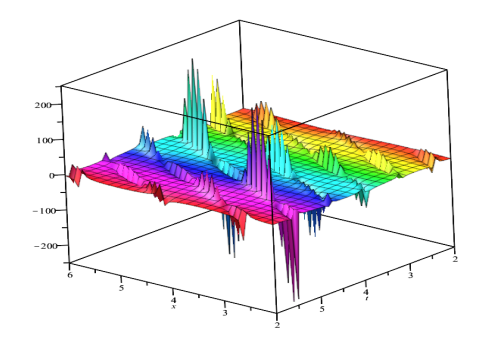
(45)
$$\begin{cases} = \left\{ \frac{-C}{\sqrt{b}} \left(-\frac{\tanh\left(\frac{\sqrt{\tanh(\eta)^{2}(-4AC)}(\eta_{0}-\eta)}{2\tanh(\eta)}\right)\sqrt{\tanh(\eta)^{2}(-4AC)}}{2\tanh(\eta)} \right)^{-1} + \left\{ \frac{A}{\sqrt{b}} \left(-\frac{\tanh\left(\frac{\sqrt{\tanh(\eta)^{2}(-4AC)}(\eta_{0}-\eta)}{2\tanh(\eta)}\right)\sqrt{\tanh(\eta)^{2}(-4AC)}}{2A\tanh(\eta)} \right) \right\} \times e^{i\psi}, \\ = \left\{ \frac{A}{\sqrt{b}} \left(-\frac{\tanh\left(\frac{\sqrt{\tanh(\eta)^{2}(-4AC)}(\eta_{0}-\eta)}{2\tanh(\eta)}\right)\sqrt{\tanh(\eta)^{2}(-4AC)}}{2A\tanh(\eta)} \right) \right\} \\ = \left\{ \frac{A}{\sqrt{b}} \left(-\frac{-\tanh\left(\frac{\sqrt{\tanh(\eta)^{2}(-4AC)}(\eta_{0}-\eta)}{2\tanh(\eta)}\right)\sqrt{\tanh(\eta)^{2}(-4AC)}}{2A\tanh(\eta)} \right\} \right\} \\ = \left\{ \frac{A}{\sqrt{b}} \left(-\frac{-\tanh\left(\frac{\sqrt{\tanh(\eta)^{2}(-4AC)}(\eta_{0}-\eta)}{2\tanh(\eta)}\right)\sqrt{\tanh(\eta)^{2}(-4AC)}}{2A\tanh(\eta)} \right\} \right\} \\ = \left\{ \frac{A}{\sqrt{b}} \left(-\frac{-\tanh\left(\frac{\sqrt{\tanh(\eta)^{2}(-4AC)}(\eta_{0}-\eta)}{2\tanh(\eta)}\right)\sqrt{\tanh(\eta)^{2}(-4AC)}} \right\} \right\} \\ = \left\{ \frac{A}{\sqrt{b}} \left(-\frac{-\tanh\left(\frac{\sqrt{\tanh(\eta)^{2}(-4AC)}(\eta_{0}-\eta)}{2\tanh(\eta)}\right)\sqrt{\tanh(\eta)^{2}(-4AC)}} \right) \right\} \\ = \left\{ \frac{A}{\sqrt{b}} \left(-\frac{-\frac{-\tanh(\eta)^{2}(-4AC)}(\eta_{0}-\eta)}{2\tanh(\eta)} \right) - \frac{-\frac{-1}{\hbar}}{4L} \right\} \right\} \\ = \left\{ \frac{A}{\sqrt{b}} \left(-\frac{-\frac{-L}{\hbar}}{4L} \right) + \frac{-L}{\hbar} \left(-\frac{-L}{\hbar} \right) + \frac{-L}{\hbar} \left(-\frac{-L}{\hbar} \left(-\frac{-L}{\hbar} \right) + \frac{-L}{\hbar} \left(-\frac{-L}{\hbar} \left(-\frac{-L}{\hbar} \left(-\frac{-L}{\hbar} \right) + \frac{-L}{\hbar} \left(-\frac{-L}{\hbar} \left(-\frac{L$$

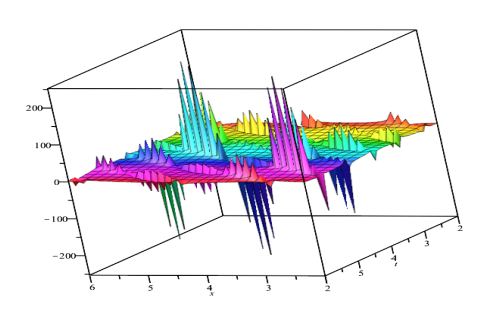
Case (4.3): When A = 0, B = 0 and $C \neq 0$,

(46)
$$\begin{cases} \Xi_{4.3} \left(\eta \right) = \frac{-C}{\sqrt{b}} \left(\frac{C(\ln(\tanh(\eta)+1)-\ln(\tanh(\eta)-1))}{2} - \eta_0 \right)^{-1} \times e^{i\psi}, \\ \eta = \left(\frac{x^{\alpha}}{\alpha} - p \frac{t^{\alpha}}{\alpha} \right), \quad \psi = \left(p \frac{x^{\alpha}}{\alpha} - \frac{(2a\delta + p^2)}{2} \frac{t^{\alpha}}{\alpha} \right), \quad \eta_0 \in \mathbb{R}. \end{cases}$$

Case (4.4): $A \neq 0, B = 0 \text{ and } C = 0,$

(47)
$$\begin{cases}
\Xi_{4.4}(\eta) = \frac{A}{\sqrt{b}} \left(\frac{1}{\eta_0 - A\xi}\right) \times e^{i\psi}, \\
\eta = \left(\frac{x^{\alpha}}{\alpha} - p\frac{t^{\alpha}}{\alpha}\right), \quad \psi = \left(p\frac{x^{\alpha}}{\alpha} - \left(\frac{-(2a\delta + p^2)}{2}\right)\frac{t^{\alpha}}{\alpha}\right), \quad \eta_0 \in \mathbb{R}.
\end{cases}$$





(A) Three-dimensional realpart

(B) Three-dimensional imaginary-part

FIGURE 8. Real and imaginary values of $\Xi_{4.1}(\eta)$ when $A=1, C=1, \eta_0=2, p=-2, b=0.8, a=0.2, \delta=0.3$ and $\alpha=1$ (periodic multi-wave).

5. Instability modulation commentary

In the following section, we operate using the linear stability analysis and perform an instability-modulated assessment on the steady solutions of Eq.(1). We assume that the permanent solutions to Eq.(1) were originally stated in the following manner:

(48)
$$\Xi(x,t) = (\sqrt{p_0} + \epsilon(x,t))e^{ibp_0x},$$

where $\epsilon(x,t)$ is a small perturbation and p_0 is the normal optical power. Putting Eq.(48) into Eq.(1) we get:

$$(49) i\mathcal{D}_t^{\alpha}\epsilon + \frac{1}{2}\left(\mathcal{D}_{xx}^{2\alpha}\epsilon + 2ibp_0D_x^{\alpha}\epsilon - b^2p_0^2(\sqrt{p_0} + \epsilon)\right) - a\delta(\sqrt{p_0} + \epsilon) - b(\sqrt{p_0} + \epsilon)^2(\sqrt{p_0} + \epsilon)^* = 0,$$

where the * indicates the conjugate to the unknown complex function ϵ which can be written as:

$$i\mathcal{D}_t^{\alpha}\epsilon + \frac{1}{2}\mathcal{D}_{xx}^{2\alpha}\epsilon + ibp_0\mathcal{D}_x^{\alpha}\epsilon - (\sqrt{p_0} + \epsilon)(\frac{b^2p_0^2}{2} + a\delta + bp_0) - bp_0(\epsilon + \epsilon^*) - b\left(2\sqrt{p_0} \mid \epsilon \mid^2 + \epsilon^2\sqrt{p_0} + \epsilon^2\epsilon^*\right) = 0.$$

After linearizing Eq. (50), we find:

$$(51) i\mathcal{D}_t^{\alpha}\epsilon + \frac{1}{2}\mathcal{D}_{xx}^{2\alpha}\epsilon + ibp_0D_x^{\alpha}\epsilon - bp_0(\epsilon + \epsilon^*) - (\sqrt{p_0} + \epsilon)(\frac{b^2p_0^2}{2} + a\delta + bp_0) = 0.$$

Suppose that the solutions of Eq.(51) take the form:

(52)
$$\epsilon(x,t) = L_1 e^{i(\lambda x + \beta t)} + L_2 e^{-i(\lambda x + \beta t)}$$

By re installing Eq.(52) into Eq.(51), we obtain:

$$-\beta L_1 e^{i(\lambda x + \beta t)} + \beta L_2 e^{-i(\lambda x + \beta t)} - \frac{1}{2} (\lambda^2 L_1 e^{i(\lambda x + \beta t)} + \lambda^2 L_2 e^{-i(\lambda x + \beta t)})$$

(53)
$$+ bp_0\lambda L_2 e^{-i(\lambda x + \beta t)} - bp_0(L_1 + L_2)e^{i(\lambda x + \beta t)} - bp_0(L_1 + L_2)e^{-i(\lambda x + \beta t)}$$
$$- (\sqrt{p_0} + L_1 e^{i(\lambda x + \beta t)} + L_2 e^{-i(\lambda x + \beta t)})(\frac{b^2 p_0^2}{2} + a\delta + bp_0) - bp_0\lambda L_1 e^{i(\lambda x + \beta t)} = 0.$$

By splitting the coefficients of $e^{i(\lambda x + \beta t)}$ and $e^{-i(\lambda x + \beta t)}$, we get:

$$-a\delta L_1 - \frac{1}{2}b^2L_1P_0^2 - b\beta L_1P_0 - 2bL_1P_0 - bL_2P_0 - \alpha L_1 + \frac{1}{2}\beta^4L_1^2 = 0,$$

$$-a\delta L_2 - \frac{1}{2}b^2L_2P_0^2 + b\beta L_2P_0 - bL_1P_0 - 2bL_2P_0 + \alpha L_2 + \frac{1}{2}\beta^4L_2^2 = 0.$$

From Eq. (54) we can easily derive the following matrix form for L_1 and L_2 :

$$\begin{pmatrix}
-\beta + \frac{\lambda^4 L_1}{2} - 2bp_0 - bp_0\lambda - \frac{b^2 p_0^2}{2} - a\delta & -bp_0 \\
-bp_0 & \beta + \frac{\lambda^4 L_2}{2} + bp_0\lambda - 2bp_0 - \frac{b^2 p_0^2}{2} - a\delta
\end{pmatrix}
\begin{pmatrix}
L_1 \\
L_2
\end{pmatrix} = \begin{pmatrix}
0 \\
0
\end{pmatrix}.$$

The coefficients matrix in Eq.(55) has a not trivial solution if the factor determinant is identical to zero. By enhancing the determinant, we acquire the results that follow:

$$a^{2}\delta^{2} - \alpha^{2} + ab^{2}\delta P_{0}^{2} + 4ab\delta P_{0} - \frac{1}{2}a\beta^{4}\delta L_{1} - \frac{1}{2}a\beta^{4}\delta L_{2} + \frac{1}{4}b^{4}P_{0}^{4} + 2b^{3}P_{0}^{3}$$

$$(56) \qquad -\frac{1}{4}b^{2}\beta^{4}L_{1}P_{0}^{2} - \frac{1}{4}b^{2}\beta^{4}L_{2}P_{0}^{2} - b^{2}\beta^{2}P_{0}^{2} + 3b^{2}P_{0}^{2} + \frac{1}{2}b\beta^{5}L_{1}P_{0} - \frac{1}{2}b\beta^{5}L_{2}P_{0}$$

$$-b\beta^{4}L_{1}P_{0} - b\beta^{4}L_{2}P_{0} - 2\alpha b\beta P_{0} + \frac{1}{2}\alpha\beta^{4}L_{1} - \frac{1}{2}\alpha\beta^{4}L_{2} + \frac{1}{4}\beta^{8}L_{1}L_{2} = 0.$$

Eq. (56) has the following solutions for β :

(57)
$$\beta = \frac{\lambda^4 L_1}{4} - \frac{\lambda^4 L_2}{4} - bp_0 \lambda \mp \frac{1}{4} \sqrt{(-\lambda^4 (L_1 + L_2) + 2bp_0 (bp_0 + 6) + 4a\delta) (-\lambda^4 (L_1 + L_2) + 2bp_0 (bp_0 + 2) + 4a\delta)}.$$

Eq.(57) guarantees the stability of the steady-state condition. If the wave number β has an imaginary portion, the steady-state solution is unstable when the disturbance rises geometrically. Nevertheless, if the wave number β is real, the state of stability is stable under tiny disturbances. Consequently, the crucial requirement for an instance of modulating instabilities that results given Eq.(56) is where:

$$(58) \qquad \left(-\lambda^4(L_1+L_2)+2bp_0(bp_0+6)+4a\delta\right)\left(-\lambda^4(L_1+L_2)+2bp_0(bp_0+2)+4a\delta\right)<0.$$

Currently, to analyze the instability modulating amplitude bandwidth, it ought to be observed the following:

(59)
$$g(\lambda) = 2Im(\beta) = \frac{\lambda^4}{2}(L_1 - L_2) - 2bp_0\lambda \mp \frac{1}{2}\sqrt{(-\lambda^4(L_1 + L_2) + 2bp_0(bp_0 + 6) + 4a\delta)(-\lambda^4(L_1 + L_2) + 2bp_0(bp_0 + 2) + 4a\delta)}$$

Thus, we are faced with the following instances: Case (1): if

(60)
$$g(\lambda) = 2Im(\beta) = \frac{\lambda^4}{2}(L_1 - L_2) - 2bp_0\lambda - \frac{1}{2}\sqrt{(-\lambda^4(L_1 + L_2) + 2bp_0(bp_0 + 6) + 4a\delta)(-\lambda^4(L_1 + L_2) + 2bp_0(bp_0 + 2) + 4a\delta)}$$

The subsequent sub-cases are accessible:

Case (1.1): If $L_1 = \frac{-2}{3}$, $L_2 = \frac{5}{3}$, $\delta = \frac{2}{5}$, b = 2, $P_1 = 1$, and $a = \frac{1}{4}$, we obtain:

$$g_{1.1}(\lambda) = \frac{-7\lambda^4}{6} - 4\lambda - \frac{1}{10}\sqrt{(-162 + 5\lambda^4)(-82 + 5\lambda^4)}.$$

Case (1.2): If
$$L_1 = \frac{3}{2}$$
, $L_2 = \frac{3}{4}$, $\delta = \frac{-1}{2}$, $b = \frac{-2}{3}$, $P_1 = \frac{1}{3}$, and $a = \frac{-3}{5}$, we obtain:

$$g_{1.2}(\lambda) = \frac{3\lambda^4}{8} + \frac{4\lambda}{9} - \frac{\sqrt{(-664 + 3645\lambda^4)(2216 + 3645\lambda^4)}}{3240}.$$

Case (1.3): If
$$L_1 = \frac{-1}{3}$$
, $L_2 = \frac{2}{5}$, $\delta = \frac{-3}{4}$, $b = \frac{-1}{2}$, $P_0 = \frac{3}{2}$, and $a = \frac{5}{4}$, we obtain:

$$g_{1.3}(\lambda) = \frac{1}{240} (-88\lambda^4 + 360\lambda - \sqrt{(675 + 8\lambda^4)(1395 + 8\lambda^4)}).$$

Case (1.4): If
$$L_1 = \frac{-1}{2}$$
, $L_2 = \frac{-5}{4}$, $\delta = \frac{1}{5}$, $b = \frac{4}{3}$, $P_1 = \frac{1}{2}$, and $a = \frac{3}{4}$, we obtain:

$$g_{1.4}(\lambda) = \frac{3\lambda^4}{8} - \frac{4\lambda}{3} - \frac{\sqrt{7(244 + 45\lambda^4)(748 + 315\lambda^4)}}{360}.$$

The figure below shows the modulation gain spectra for the above sub-cases for the mentioned values in the legend.

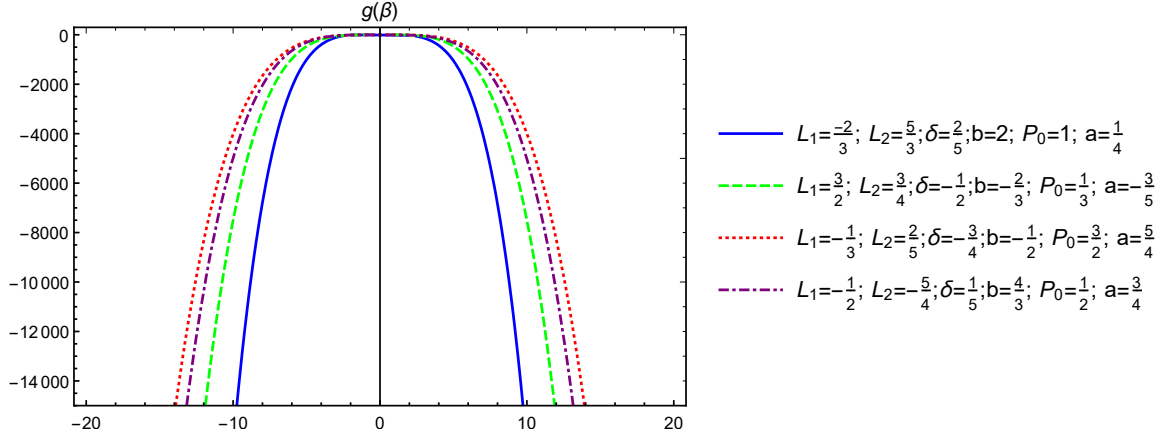


FIGURE 9. The standard-GVD domain instability modulating gained spectrum for various values in Eq.(60).

Case (2): if

(61)
$$g(\lambda) = 2Im(\beta) = \frac{\lambda^4}{2}(L_1 - L_2) - 2bp_0\lambda + \frac{1}{2}\sqrt{(-\lambda^4(L_1 + L_2) + 2bp_0(bp_0 + 6) + 4a\delta)(-\lambda^4(L_1 + L_2) + 2bp_0(bp_0 + 2) + 4a\delta)}.$$

The next sub-cases have been achieved:

Case (2.1): If $L_1 = \frac{2}{3}$, $L_2 = \frac{5}{3}$, $\delta = \frac{-2}{5}$, $b = \frac{2}{3}$, $P_0 = \frac{1}{3}$, and $a = \frac{1}{4}$, we obtain:

$$g_{2.1}(\lambda) = -\frac{\lambda^4}{2} - \frac{4\lambda}{9} + \frac{\sqrt{7(135\lambda^4 - 34)(945\lambda^4 - 958)}}{810}.$$

Case (2.2): If $L_1 = \frac{3}{2}$, $L_2 = \frac{3}{4}$, $\delta = -\frac{1}{2}$, $b = -\frac{2}{3}$, $p_0 = \frac{1}{3}$, and $a = -\frac{3}{5}$, we obtain:

$$g_{2.2}(\lambda) = \frac{3\lambda^4}{8} + \frac{4\lambda}{9} + \frac{\sqrt{(3645\lambda^4 - 664)(3645\lambda^4 + 2216)}}{3240}$$

Case (2.3): If $L_1 = -\frac{1}{3}$, $L_2 = -\frac{2}{5}$, $\delta = -\frac{3}{4}$, $b = -\frac{1}{2}p_0' = \frac{3}{2}$, and $a = \frac{5}{4}$, we obtain:

$$g_{2.3}(\lambda) = \frac{\lambda^4}{30} + \frac{3\lambda}{2} + \frac{\sqrt{(88\lambda^4 - 675)(88\lambda^4 - 1395)}}{240}.$$

Case (2.4): If
$$L_1 = -\frac{1}{2}$$
, $L_2 = -\frac{5}{4}$, $\delta = -\frac{1}{5}$, $b = \frac{4}{3}$, $p_0 = \frac{1}{2}$, and $a = \frac{3}{4}$, we obtain:
$$g_{2.4}(\lambda) = \frac{3\lambda^4}{8} - \frac{4\lambda}{3} + \frac{\sqrt{7(45\lambda^4 + 76)(315\lambda^4 + 1492)}}{360}.$$

The illustration below displays the modulation gain spectra for the aforementioned sub-cases, using the values specified in the legend.

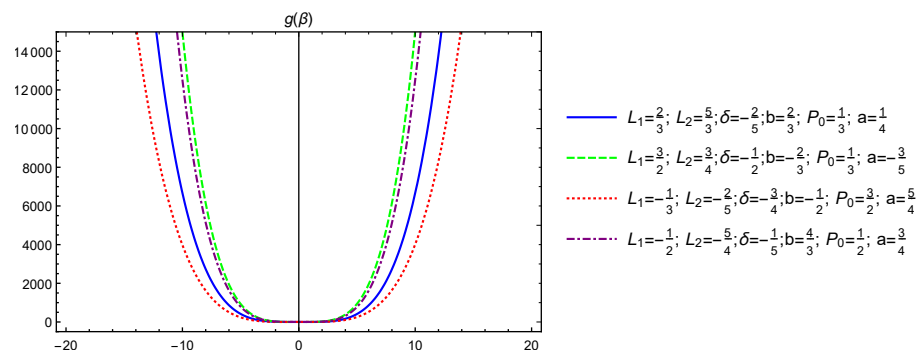


FIGURE 10. The standard-GVD domain instability modulating gained spectrum for various values in Eq.(61).

6. Conclusion

This work addressed the nonlinear Schrödinger's equation with a δ -potential, where δ represents a Dirac measure located at the origin. The present work presents the use of bifurcation theory to examine the bifurcation and phase picture of the solutions. In addition, the modified Cham approach has been used to get numerous traveling wave solutions, such as kink, periodic multi-wave soliton, and coindal waves. The identified solutions have been visually shown to enhance the readers' comprehension of their physical properties. In addition, we have used the linear stability analysis method to conduct an examination of instability modulation for stationary solutions. Our technique has been determined to be practical and adaptable to many mathematical, physical, and engineering models. Compared to previous studies our results are original. The graphics representations clarify the evaluation of the work. The phase portraits of the planar system in two and three dimensions have been illustrated by Figure (1), which implies that E_0 is a saddle point and we can infer that the fixed point E_0 is unstable. In Figure (2), the fact E_0 is a center because λ_1 and λ_2 are two purely imaginary numbers and stable in the sense of Lyapunov, which implies that we have two unstable saddle fixed points. The exact solutions to δ -Schrödinger's equation by using the improved Cham method presenting kink wave solution by Figure (3), periodic multi-wave solitons by Figure (4), kinky-periodic lump wave by Figure (5), continual wave solutions by Figure (6), periodic singular solutions by Figure (7), periodic multi-wave by Figure (8), and the instability modulation gain spectra in the normal-GVD regime for the steady-state solutions by Figures (9), (10).

REFERENCES

- [1] L. Alhakim, A. Moussa, The double auxiliary equations method and its application to space-time fractional nonlinear equations, J. Ocean Eng. Sci. 4 (2019), 7–13.
- [2] B. Gasmi, L. Alhakim, Y. Mati, A. Moussa, A. Akgül, R. Wannan, J. Asad, Novel exact and solitary wave solutions for the time-fractional nonlinear maccari's system, Contemp. Math. (2023), 937–950.

- [3] B. Gasmi, A. Moussa, Y. Mati, L. Alhakim, H. M. Baskonus, Bifurcation and exact traveling wave solutions to a conformable nonlinear schrödinger equation using a generalized double auxiliary equation method, Opt. Quantum Electron. 56 (2024), 18.
- [4] A. A. Moussa, L. A. Alhakim, Fractional $\exp(-\varphi(\xi))$ -expansion method and its application to space—time nonlinear fractional equations, Aust. J. Math. Anal. Appl. 17 (2020), 1–15.
- [5] B. Gasmi, A. Moussa, Y. Mati, L. Alhakim, A. Akgül, Solving nonlinear partial differential equations using a novel cham method, J. Taibah Univ. Sci. 17 (2023), 2272728.
- [6] B. Gasmi, A. A. Moussa, Y. Mati, L. A. Alhakim, A. Akgül, New exact traveling wave solutions to the kawahara equation using the tanh (ξ) expansion method, Int. J. Appl. Comput. Math. 9 (2023), 98.
- [7] S. Sivasundaram, A. Kumar, R. K. Singh, On the complex properties to the first equation of the kadomtsev-petviashvili hierarchy, Int. J. Math. Comput. Eng. (2024).
- [8] A. Hussain, H. Ali, F. Zaman, N. Abbas, New closed form solutions of some nonlinear pseudo-parabolic models via a new extended direct algebraic method, Int. J. Math. Comput. Eng. 2 (2023), 35–58.
- [9] H. M. Baskonus, T. A. Sulaiman, H. Bulut, T. Aktürk, Investigations of dark, bright, combined dark-bright optical and other soliton solutions in the complex cubic nonlinear schrödinger equation with δ-potential, Superlattices Microstruct. 115 (2018), 19–29.
- [10] R. Khalil, M. Al Horani, A. Yousef, M. Sababheh, A new definition of fractional derivative, J. Comput. Appl. Math. 264 (2014), 65–70.
- [11] D. Baleanu, M. Inc, A. I. Aliyu, A. Yusuf, Optical solitons, nonlinear self-adjointness and conservation laws for the cubic nonlinear schrödinger's equation with repulsive delta potential, Superlattices Microstruct. 111 (2017), 546–555.
- [12] B. Cheng, Y.-M. Chen, C.-F. Xu, D.-L. Li, X.-G. Deng, Nonlinear schrödinger equation with a Dirac delta potential: finite difference method, Commun. Theor. Phys. 72 (2020), 025001.
- [13] P. Deift, J. Park, Long-time asymptotics for solutions of the NLS equation with a delta potential and even initial data, Int. Math. Res. Not. 2011 (2011), 5505–5624.
- [14] Y.-X. Li, E. Celik, J. L. Guirao, T. Saeed, H. M. Baskonus, On the modulation instability analysis and deeper properties of the cubic nonlinear schrödinger's equation with repulsive δ -potential, Results Phys. 25 (2021), 104303.
- [15] J. Bai, Multi-symplectic Runge-Kutta-Nyström methods for nonsmooth nonlinear schrödinger equations, J. Math. Anal. Appl. 444 (2016), 721–736.
- [16] S. Masaki, J. Murphy, J.-I. Segata, Modified scattering for the one-dimensional cubic NLS with a repulsive delta potential, Int. Math. Res. Not. 2019 (2019), 7577–7603.
- [17] J. Holmer, J. Marzuola, M. Zworski, Soliton splitting by external delta potentials, J. Nonlinear Sci. 17 (2007), 349–367.
- [18] J.-I. Segata, Final state problem for the cubic nonlinear schrödinger equation with repulsive delta potential, Commun. Partial Differ. Equ. 40 (2015), 309–328.
- [19] K. A. Muhamad, T. Tanriverdi, A. A. Mahmud, H. M. Baskonus, Interaction characteristics of the Riemann wave propagation in the (2+1)-dimensional generalized breaking soliton system, Int. J. Comput. Math. 100 (2023), 1340–1355.
- [20] A. A. Mahmud, T. Tanriverdi, K. A. Muhamad, H. M. Baskonus, Characteristic of ion-acoustic waves described in the solutions of the (3+1)-dimensional generalized Korteweg-de Vries-Zakharov-Kuznetsov equation, J. Appl. Math. Comput. Mech. 22 (2023), 36–48.
- [21] H. M. Baskonus, A. A. Mahmud, K. A. Muhamad, T. Tanriverdi, A study on Caudrey-Dodd-Gibbon-Sawada-Kotera partial differential equation, Math. Methods Appl. Sci. 45 (2022), 8737–8753.
- [22] H. M. Baskonus, A. A. Mahmud, K. A. Muhamad, T. Tanriverdi, W. Gao, Studying on Kudryashov-Sinelshchikov dynamical equation arising in mixtures liquid and gas bubbles, Therm. Sci. 26 (2022), 1229–1244.
- [23] A. A. Mahmud, T. Tanriverdi, K. A. Muhamad, H. M. Baskonus, Structure of the analytic solutions for the complex non-linear (2+1)-dimensional conformable time-fractional schrödinger equation, Therm. Sci. 27 (2023), 211–225.

- [24] A. J. M. Jawad, A. Moussa, L. Alhakim, Bifurcation and exact traveling wave solutions for Kodomtsev-Petviashvili equation, J. Mech. Eng. Res. Dev. 44 (2021), 177–187.
- [25] T. Han, L. Zhao, Bifurcation, sensitivity analysis and exact traveling wave solutions for the stochastic fractional Hirota–Maccari system, Results Phys. 47 (2023), 106349.
- [26] C.-Y. Qin, Modulation instability analysis, solitary wave solutions, dark soliton solutions, and complexitons for the (3+1)-dimensional nonlinear schrödinger equation, J. Math. 2022 (2022), 4689857.
- [27] M. Arshad, A. R. Seadawy, D. Lu, W. Jun, Modulation instability analysis of modify unstable nonlinear Schrödinger dynamical equation and its optical soliton solutions, Results Phys. 7 (2017), 4153–4161.
- [28] S. ur Rehman, J. Ahmad, Modulation instability analysis and optical solitons in birefringent fibers to RKL equation without four wave mixing, Alex. Eng. J. 60 (2021), 1339–1354.
- [29] K. K. Al-Kalbani, K. S. Al-Ghafri, E. V. Krishnan, A. Biswas, Optical solitons and modulation instability analysis with Lakshmanan-Porsezian-Daniel model having parabolic law of self-phase modulation, Math. 11 (2023), 2471.
- [30] G. Akram, M. Sadaf, S. Arshed, U. Ejaz, Travelling wave solutions and modulation instability analysis of the nonlinear Manakov-system, J. Taibah Univ. Sci. 17 (2023), 2201967.
- [31] A. I. Aliyu, A. Yusuf, D. Baleanu, et al., Optical solitons and modulation instability analysis to the quadratic-cubic nonlinear schrödinger equation, Nonlinear Anal. Model. Control 24 (2019), 20–33.
- [32] A. A. Mahmud, H. M. Baskonus, T. Tanriverdi, K. A. Muhamad, Optical solitary waves and soliton solutions of the (3+1)-dimensional generalized Kadomtsev–Petviashvili–Benjamin–Bona–Mahony equation, Comput. Math. Math. Phys. 63 (2023), 1085–1102.
- [33] A. A. Mahmud, Considerable traveling wave solutions of a generalized Hietarinta-type equation, Int. J. Math. Comput. Eng. 3 (2024), 185–200.
- [34] A. A. Mahmud, T. Tanriverdi, K. A. Muhamad, Exact traveling wave solutions for (2+1)-dimensional Konopelchenko-Dubrovsky equation by using the hyperbolic trigonometric functions methods, Int. J. Math. Comput. Eng. 1 (2023), 11–24.
- [35] A. A. Mahmud, K. A. Muhamad, T. Tanriverdi, H. M. Baskonus, An investigation of Fokas system using two new modifications for the trigonometric and hyperbolic trigonometric function methods, Opt. Quantum Electron. 56 (2024), 717.
- [36] T. Tanriverdi, H. M. Baskonus, A. A. Mahmud, K. A. Muhamad, Explicit solution of fractional order atmosphere-soil-land plant carbon cycle system, Ecol. Complex. 48 (2021), 100966.
- [37] A. Kumar, S. Kumar, Dynamic nature of analytical soliton solutions of the (1+1)-dimensional Mikhailov-Novikov-Wang equation using the unified approach, Int. J. Math. Comput. Eng. 1 (2023), 217–228.